Steck, A. J., & Appel, S. H. (1974) *J. Biol. Chem. 249*, 5416.
Sulakhe, P. V., Petrali, E. H., & Thiessen, B. J. (1978) *Neurosci. Abstr. 4*, 249.
Sulakhe, P. V., Petrali, E. H., Thiessen, B. J., & Davis, E. R. (1980) *Biochem. J. 186*, 469.
Teo, T. S., & Wang, J. H. (1973) *J. Biol. Chem. 248*, 5950.
Teo, T. S., Wang, T. H., & Wang, J. H. (1973) *J. Biol. Chem. 248*, 588.
Waehneldt, T. V. (1977) *Adv. Exp. Med. Biol. 100*, 117.
Waehneldt, T. V. (1978) *Brain Res. Bull. 3*, 37.
Waehneldt, T. V., Matthieu, J.-M., & Neuhoff, V. (1977) *Brain Res. 138*, 29.
Wang, J. H., & Desai, R. (1977) *J. Biol. Chem. 252*, 4175.
Wang, J. H., & Waisman, D. M. (1979) *Curr. Top. Cell. Regul. 15*, 47.
Yourist, J. E., Ahmad, F., & Brady, A. H. (1978) *Biochim. Biophys. Acta 522*, 452.
Zimmerman, A. W., Quarles, R. H., Webster, H. DeF., Matthieu, J. M., and Brady, R. O. (1975) *J. Neurochem. 25*, 749.

Conformational Transitions in the Subfragment-2 Region of Myosin†

C. A. Swenson* and P. A. Ritchie

ABSTRACT: A differential scanning calorimeter was used to observe thermally induced conformational transitions in subfragment 2 (S-2) of myosin. In addition to an endotherm for the major transition which had been observed by several other methods earlier, a small broad endotherm was noted with a T_m of 41 °C. By analysis of the heat capacity profiles of long and short S-2, this endotherm was assigned to the hinge region. Comparison of the amino acid compositions of S-2 and tropomyosin showed them to be remarkably similar, and in view of their similar behavior in calorimetric studies, it is apparent that interactions stabilizing the coiled-coil structure of S-2 are a hydrophobic interface supported by charged interaction spanning the groove as was suggested for tropomyosin by McLachlan and Stewart [McLachlan, A. D., & Stewart, M. (1975) *J. Mol. Biol. 98*, 293–304].

The multifunctional role of myosin in the molecular mechanism of muscle contraction requires that it contain structural domains (Kirschner & Bisswanger, 1976) suited to each function. Two structural features are obvious: (1) the globular head (subfragment 1), which contains the sites for ATP hydrolysis and actin binding, and (2) the coiled-coil rod, which contains the sites of the molecular interactions which direct the proper self-assembly of myosin molecules into the thick filament and support tension. Association of the various functions with a specific part of the structure has been achieved by enzymatic cleavage. Myosin can be cleaved into subfragment 1 (S-1)[1] and rod by several enzymes (Bâlint et al., 1975; Weeds & Taylor, 1975; Weeds & Pope, 1977). The rod portion can be enzymatically cleaved to yield subfragment 2 (S-2) and light meromyosin (LMM). The susceptibility of these two regions of myosin to enzymatic cleavage has led to the hypothesis that they are functional hinges in the context of the sliding filament model of muscle contraction (Huxley & Hanson, 1954). Current theories are considering changes in conformation of these regions (Harrington, 1971) and changes in relative orientation (Huxley, 1969; Huxley & Simmons, 1971) between the domains as events which provide a molecular basis for the generation of tension in skeletal muscle. The nature of these processes and their coupling to the hydrolysis of ATP is poorly, if at all, understood.

Considerable attention has been focused recently on S-2 (Harrington, 1979a,b). In current models for contraction, it has variously been suggested as (a) a rigid connecting link between LMM and S-1 which because of the hinge regions allows S-1 to engage actin to form a cross bridge (Huxley, 1969), (b) a series-elastic element which is stretched upon tension generation by rotation of S-1 at the actin-S-1 interface and then transmits this force to the myosin thick filament (Huxley & Simmons, 1971), and (c) a source of tension generation via a helix–coil transition in a portion of the coiled-coil structure (Harrington, 1971, 1979a,b). The recent work of Harrington and collaborators provides support for a helix–coil transition in S-2 as the origin of the contractile force. These workers have carefully characterized a less degraded form of S-2 and found that, in contrast to previous studies with shorter S-2, this long S-2 self-associates at physiological ionic strengths (Sutoh et al., 1978). In earlier experiments, Tsong et al. (1979) have shown that the rate constants for opening and closing the coiled-coil strucuture of S-2 are in the same range observed for the quick-recovery process in muscle fibers (Huxley & Simmons, 1971). From these and other observations, these authors have suggested a model for contraction in which S-2 is in close contact with the thick filament in the relaxed state. Following S-1 binding to actin, S-2 is released from the thick filament and contracts via a helix–coil transition to generate tension (Harrington, 1979b). In this paper we report on the properties of the helix–coil conformational transitions of S-2 as measured by a differential scanning calorimeter. Evidence is presented for a second helix–coil transition which is assigned to the hinge region of S-2.

Materials and Methods

Myosin was prepared from rabbit skeletal muscle and characterized as described earlier (Goodno & Swenson, 1975a,b). It was stored at 4 °C as a pellet which was the

† From the Department of Biochemistry, University of Iowa, Iowa City, Iowa 52242. *Received April 28, 1980.* This work was supported by grants from National Institutes of Health (HL14388) and the National Science Foundation (PCM77-08087).

[1] Abbreviations used: S-1, subfragment 1 of myosin; S-2, subfragment 2 of myosin; LMM, light meromyosin; HMM, heavy meromyosin; NaDodSO$_4$, sodium dodecyl sulfate.

0006-2960/80/0419-5371$01.00/0

precipitate obtained when the ammonium sulfate concentration was raised from 35 to 45% of saturation. For some preparations the crude myosin was sieved on Bio-Gel A 1.5 M; however, no improvement was noted in the quality of the helical myosin fragments. The calcium and EDTA ATPase activities were assayed under the conditions of Kielley & Bradley (1956) and Kielley et al. (1956) and were respectively 0.90 ± 0.02 (SEM) and 3.04 ± 0.08 (SEM) μmol of P_i min^{-1} (mg of protein)$^{-1}$ for 30 recent laboratory preparations.

Long S-2 was prepared from myosin in two chymotryptic-digestion steps. Myosin was digested with chymotrypsin according to the procedure of Weeds & Taylor (1975) to produce heavy meromyosin (HMM). Long S-2 was prepared from HMM, and short S-2 was prepared from long S-2 by the procedures of Sutoh et al. (1978).

The purity of myosin, HMM, and S-2 was checked by sodium dodecyl sulfate ($NaDodSO_4$)–polyacrylamide gel electrophoresis. Subfragment 2 was also run on native gels. Myosin and HMM showed the usual pattern of peptides (Weeds & Pope, 1977). Long S-2 showed a major peak at a position corresponding to 60 000 g/mol with minor bands at 72 000 and 45 000 g/mol, in agreement with Weeds & Pope (1977) and Sutoh et al. (1978). We were not successful in removing the contaminating peaks by the column procedure noted by Sutoh et al. (1978) or by repeated dialysis to low ionic strength. Native gels showed predominantly a single band which suggests that chymotryptic digestion likely results in nicking of a single strand of the coiled-coil structure in a small fraction of the molecules and that noncovalent interactions keep these molecules intact. Electrophoretic studies ($NaDodSO_4$–polyacrylamide gel electrophoresis) of short S-2 indicated a molecular weight of 35 000 g mol^{-1}. The homogeneity of S-2 was a major concern for these studies; we estimate that the purity of our samples was greater than 90%. The data for this work were taken on ten different samples of long S-2 and three samples of short S-2, and similar results were obtained in each case. When a sample contained large amounts of impurities, greater than 10% by $NaDodSO_4$–polyacrylamide gel electrophoresis, the heat capacity profiles were noted to be abnormal and discarded.

Protein concentrations were determined by the biuret method with bovine serum albumin as a standard and by the known ultraviolet extinction coefficients: $\epsilon^{1\%}_{1cm}$ of 5.5, 6.47, and 0.7, respectively, for myosin, HMM, and S-2 (Godfrey & Harrington, 1970; Young et al., 1965; Lowey et al., 1969).

Calorimetric experiments were performed in a heat capacity calorimeter, Model MC-1, manufactured by Microcal, Inc., Amherst, MA. The excess heat capacity of a degassed 1-mL sample was scanned over the temperature range from ~5 to 80 °C at a rate of 1 °C/min with protein concentrations which ranged from 1 to 6 mg/mL.

The characteristic melting temperature, T_m, was obtained as the maximum of the transition endotherm. Enthalpies of the conformational transitions were determined by integration of the area under the curves after base lines were drawn. For this procedure, the native and denatured base lines were linearly extrapolated to intersect a vertical line at the T_m, and the area above these base lines and enclosed by the curve of the endotherm was taken as proportional to the transition enthalpy (Jackson & Brandts, 1970). Characteristic melting temperatures were reproducible to ±0.3 °C and the enthalpies for transitions between states were reproducible to ±20% by using these procedures.

Resolution of the overlapping endotherms was attempted by using a Du Pont 310 curve resolver. Qualitative results are obtained due to the uncertainty in the base line and curve shape.

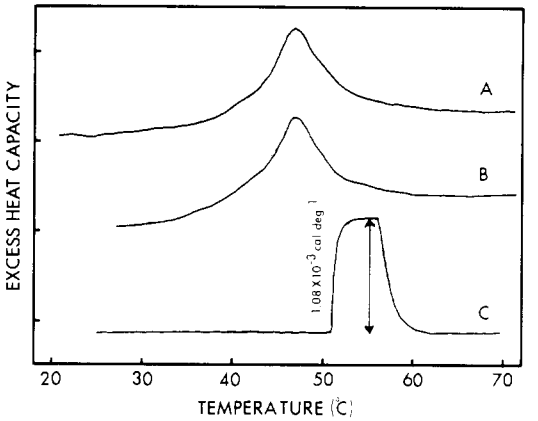

FIGURE 1: DSC scans of subfragment-2; reversibility, calibration: (A) 2.1 mg/mL protein in 0.2 M KCl and 20 mM sodium phosphate, pH 7.0; (B) remelt of sample in (A) after cooling to 0 °C; (C) base line for the buffer as in (A) with superimposed calibration heat of 1.08 mcal/deg.

Calibration of the ordinate was achieved by injecting heat at a known rate (1.08 mcal min^{-1}) into the reference cell for compensation by the heaters of the sample cell and quantitating the output signal.

Results

The excess heat capacity as measured by a differential scanning calorimeter can be partitioned into contributions from the intrinsic properties of a state and from transitions between states. The former contributes to the base line and the latter to the endotherm(s) which are superimposed on the base line. In Figure 1A is shown a typical heat capacity profile for long subfragment-2 of myosin in a solvent consisting of 0.2 M KCl and 20 mM sodium phosphate buffer, pH 7.2. For long S-2 a single major transition is observed with a T_m of 46.8 °C. The pretransition base line shows a positive slope due to the increase in heat capacity of the native protein with temperature. At temperatures above the transition a similar but somewhat smaller positive slope is noted for the base line. In Figure 1B is presented the heat capacity profile obtained when the sample used to obtain 1A was cooled to ~0 °C and remelted. Similar results were obtained for remelts of long S-2 in the pH range 5.5–8 and for salt concentrations in the range 0.1–0.6 M. An instrument base line as shown in Figure 1C was obtained when the buffer used in Figure 1A was substituted for the protein solution in the sample cell. Superimposed on the instrument base line is the excess signal observed when heat is added to the reference cell at a rate of 1.08 mcal min^{-1} (calibration).

Figure 2 shows the effect of pH on the heat capacity profile. The midpoint (T_m) of the major transition increases with decreasing pH. Although measurements are not possible in the vicinity of the isoelectric point, at pH values below the isoelectric point the melting temperature is greater than 60 °C. It is apparent that shoulders are present at pH 6.2 on both the high- and low-temperature sides of the major transition. These shoulders appeared in all preparations of long S-2. The transition which gives rise to the endotherm on the low-temperature side of the main endotherm has a small pH dependence and is masked by the major transition at high pHs. The major transition and the transition on its high-temperature side appear to have a similar dependence on pH.

Figure 3 summarizes the dependence of the T_m of the major endotherm on pH and salt concentration. The region of S-2 that gives rise to the observed endotherm is in general stabilized

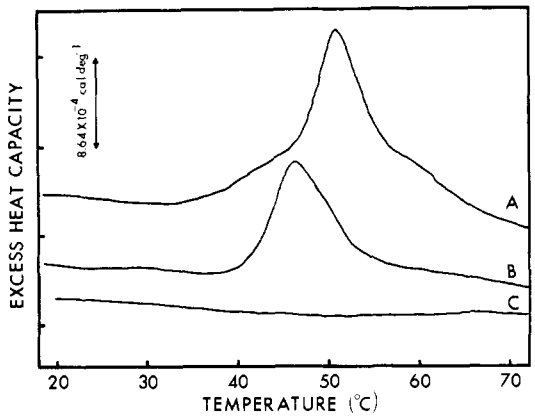

FIGURE 2: DSC scans of subfragment-2; pH dependence: (A) 4.4 mg/mL protein, no KCl, 20 mM sodium phosphate, pH 6.2; (B) 4.3 mg/mL protein, no KCl, 20 mM sodium phosphate, pH 7.6; (C) base line, 20 mM sodium phosphate, pH 6.2.

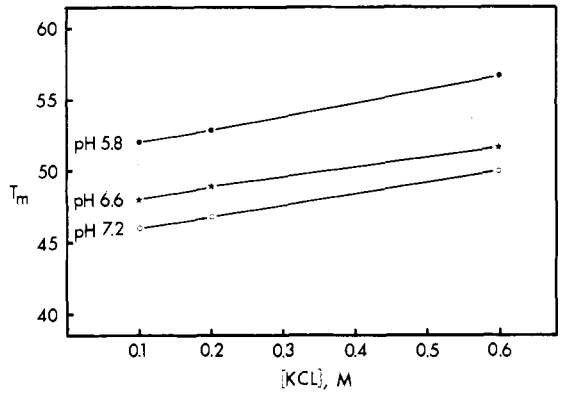

FIGURE 3: Dependence of T_m on KCl concentration: (●) pH 5.8; (☆) pH 6.6; (○) pH 7.2.

by lowering the pH and increasing the salt concentration. Over the pH range 5.5–7.5 (20 mM sodium phosphate) and a salt concentration range 0.1–0.6 M, T_m ranges from 46 to 57 °C. Unbuffered solutions gave similar results.

The calorimetric enthalpy for the major transition ranged from 2.2 ± 0.4 cal g^{-1} at pH 7.4 (T_m = 46 °C) to 3.2 ± 0.6 cal g^{-1} at pH 6.2 (T_m = 52 °C) in 0.2 M salt. This enthalpy is essentially a linear function of T_m. The ΔC_p, determined as the difference in the extrapolated native and denatured base lines at the T_m, was 0.06 ± 0.03 cal g^{-1} deg^{-1}. Temperature variation of the measured enthalpies corresponded to a ΔC_p of 0.17 ± 0.05 cal g^{-1} deg^{-1}. The large errors associated with these numbers arise from the usual base line and sampling errors plus the difficulty in curve resolution of the small transition which can be resolved from the major transition at pH 6.2 while at pH 7.4 it is either absent or coincident with it. Our best estimate of the enthalpy of the small transition is 0.6 ± 0.3 cal g^{-1} at pH 6.2, and it decreases with increasing pH.

Digestion of long S-2 with trypsin produces short S-2 (70 000 g mol^{-1}). This fragment lacks the hinge region adjacent to the LMM junction (Sutoh et al., 1978). The heat capacity profile of short S-2 (curve C) is compared to those of long S-2 (curves A and B) in Figure 4. It is apparent that a small endotherm is present on the low-temperature side of the major transition of long S-2 and that some asymmetry is present on the high-temperature side. The low-temperature transition is broad with a maximum at 42 °C at pH 7.2 and 0.6 M salt. As the pH is decreased to 6.6, the endotherm broadens and the T_m decreases slightly. At pH 5.8 the endotherm is sufficiently broad so that it disappears into the base line. This transition appears at all salt concentrations but is more clearly resolved in high salt which shifts the major endotherm to higher temperatures.

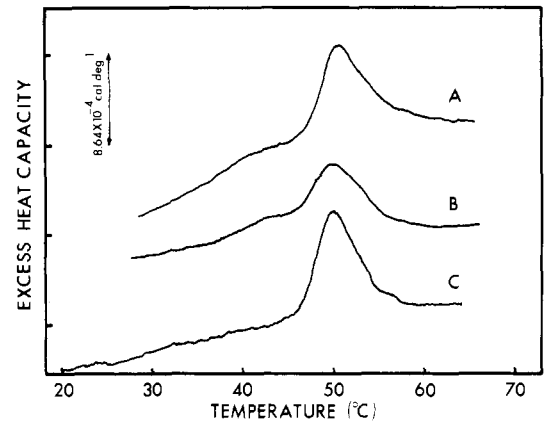

FIGURE 4: DSC scans of long and short subfragment-2: (A) Long S-2, 2.0 mg/mL protein, 0.6 M KCl, 20 mM sodium phosphate, pH 6.6; (B) long S-2, 2.0 mg/mL protein, 0.6 M KCl, and 20 mM sodium phosphate, pH 7.2; (C) short S-2, 1.28 mg/mL protein, 0.5 M KCl, and 20 mM sodium phosphate, pH 7.0, ordinate scale expansion ×2.

In short S-2 the low-temperature endotherm is absent, and some asymmetry is still apparent on the high-temperature side of the major endotherm. The pH and salt dependence of the T_m of the major endotherm in short S-2 is the same as was noted for long S-2. The enthalpy of this transition is 2.0 ± 0.2 cal g^{-1} in a solvent consisting of 0.5 M KCl and 10 mM sodium phosphate, pH 7.0.

Discussion

Several hypotheses for energy transduction in the actomyosin ATPase system involve subfragment 2 either as a supporting structural or as a transducing element. Numerous studies (Burke et al., 1973; Highsmith et al., 1977; Harvey & Cheung, 1977) have been performed to assess the flexibility of S-2, LMM, and rod and have incorporated the experimental results into a basis for the cross bridge mechanisms of transduction. With the same goal in mind, several laboratories have studied the conformational states available to the helical fragments of myosin (Burke et al., 1973; Jacobson & Henderson, 1977; Goodno & Swenson, 1975a,b; Goodno et al., 1976). These physical studies and enzymatic studies lead to the conclusion that the myosin rod is composed of a rigid LMM segment which is joined to a somewhat flexible S-2 segment. Both regions undergo thermally induced conformational transitions. The flexible portion in S-2 is adjacent to the junction of S-2 and LMM. To further elucidate this picture, we present data from heat capacity calorimetry. This technique has definite advantages over the pH and spectroscopic methods. For these methods it is difficult to locate conformational transitions on the progress curve, and as a result the first derivative is often plotted vs. the variable to objectively determine T_m and the number of transitions. The output from a heat capacity calorimeter is inherently the derivative curve, and thus it is easy to detect multiple transitions or changes in T_m due to changes in solution variables. As an example, careful studies of myosin rod using optical rotatory dispersion (ORD) have shown that it undergoes two between-state transitions. Heat capacity calorimetry shows that this structure undergoes at least six transitions, two of which can be correlated with the transitions observed spectroscopically (C. A. Swenson and T. Nguyen, unpublished results). A disadvantage of the calorimetric method is that

more sample is required (generally 2–3 mg) than for ORD or circular dichroism measurements. It is also necessary that the transitions be inherently cooperative; however, this seems to be true for the helical fragments of myosin. Finally, it is clear that heat capacity calorimetry provides a direct measure of the enthalpy, which with T_m characterizes the reversible between-state transitions.

The observation of a large endotherm with a T_m of 46.8 °C for long S-2 in 0.2 M KCl and 20 mM sodium phosphate, pH 7.0, is in good agreement with the conformational transition detected in earlier studies (Burke et al., 1973; Goodno et al., 1976). Correlation of the observations from the various techniques is supported by an identical pH and ionic strength dependence of the T_m. New features in the thermal unfolding of S-2 observed in this work are the weak transitions noted at 41 and 55 °C (shoulder) in 20 mM sodium phosphate, pH 6.2 (Figure 2), flanking the main transition. Neither of these transitions was noted with the pH or spectroscopic methods. The transition at 41 °C is broad and can be associated with the slow decrease in helicity prior to the major transition observed in optical rotation studies (Tsong et al., 1979). Thus it likely arises from the melting of a small, poorly organized region of helix. LMM does have an endotherm at ~41 °C (C. A. Swenson and T. Nguyen, unpublished results). However, this endotherm is sharp; furthermore, no LMM contaminant was noted on the $NaDodSO_4$ gels, so it is likely that this endotherm and the endotherm at 55 °C arise from melting of helical regions which are a constitutive part of long S-2.

The elevation in T_m (stability) observed on lowering the pH or increasing the salt concentration suggests that ionic interactions are important in maintaining the integrity of this coiled-coil structure. Observations made on tropomyosin, another coiled-coil structure of known sequence, have shown similar results (D. L. Williams and C. A. Swenson, unpublished results). In both cases it is clear that the sequence must be appropriate to stabilize the coiled-coil structure as opposed to one that would dictate a globular structure. An extensive analysis has been performed by McLachlan & Stewart (1975) on the interactions in the coiled-coil structure of tropomyosin using the known sequence and chemical and stereochemical arguments. First, at the interface between the two helices, residues with apolar side chains (Ala, Leu, Ile, Val) were found in 130 of the possible 162 positions. In positions spanning the groove between the two helices, charged amino acids were in 116 of 162 positions. Of these, 70 are acidic and 46 are basic so the helical interface has an excess of negative charge. As suggested by McLachlan & Stewart (1975), it is likely the stability in high salt is due to screening of the excess negative charge which tends to destabilize the structure. Decreases in stability above pH 7.0 occur because of the loss of favorable electrostatic interactions while increases in stability at low pH result from a decrease in the excess of acidic groups. Comparisons of the compositions of S-2 or LMM with that of tropomyosin show them to be quite similar: e.g. (amino acid, residues/10^5 g of S-2, residues/10^5 g of tropomyosin), Ala, 87, 102; Leu, 99, 96; Ile, 34, 34; Val, 24, 30; Glu, 242, 216; Asp, 87, 87; Lys, 121, 115; Arg, 37, 42. This composition is then seemingly characteristic of the coiled-coil structure wherein these residues compose 90% of the sequence. Thus our observations that the pH and ionic strength dependence of T_m for S-2 and tropomyosin are similar and that the compositions are similar strongly suggest that the coiled-coil structure of S-2 is stabilized by the same interactions as tropomyosin, namely, a hydrophobic interface with charged interactions across the cleft between the helices.

The transition enthalpy is the parameter of greatest interest measured in this work. Approximately 3 cal of heat was absorbed per g of protein in the major transition of S-2. Potekhin et al. (1979) have studied the thermal unfolding of myosin rod and LMM. Although the endotherm corresponding to S-2 unfolding was not observed directly, an estimate of the enthalpy is obtained from the difference between these two myosin fragments. When their measured enthalpy and the molecular weight for long S-2 are used (Sutoh et al., 1978), the enthalpy for the transition in S-2 is ~2 cal g^{-1}, which is in substantial agreement with the result of this study. These values for S-2 are lower than the 4–10 cal g^{-1} observed for a series of globular proteins (Privalov & Khechinashvili, 1974) and less than the average value of 5.6 cal g^{-1} obtained for the transitions observed in the similar coiled-coil structure tropomyosin and the other transition in myosin rod (Potekhin & Privalov, 1978; Potekhin et al., 1979). Since parallel measurements of molar ellipticity show that the α-helical structure is completely destroyed (Tsong et al., 1979), the smaller measured enthalpy suggests that the coiled-coil structure of S-2 is inherently of lower stability. It should be noted that a different treatment of the base-line corrections and sample heterogeneity could make an appreciable contribution to the measured enthalpies.

The increase in transition enthalpy with temperature corresponds to a ΔC_p of ~0.2 cal deg^{-1} g^{-1}. This value of ΔCp is somewhat larger than is obtained from the difference in extrapolated native and denatured base lines, suggesting that the transition enthalpy is not solely a function of temperature but also depends on pH. This finding is in contrast to the observations of Privalov & Khechinashvili (1974) on globular proteins wherein these two ΔC_p's were identical. These authors suggested that the enthalpy increase arises from a decrease in the ability of the amino acid side chains to form compensatory interactions, specifically hydrogen bonds and hydrophobic interactions, with the solvent as the temperature increases. A similar mechanism may be responsible for the temperature dependence of the transition enthalpies observed for the coiled-coil structure of S-2.

The broad minor transition at 41 °C has an enthalpy, 0.4 cal g^{-1}, which is approximately one-fifth that of the major transition. With the assumption that the ΔH per residue is similar for all the residues, this enthalpy corresponds to ~90 residues per chain of coiled-coil structure. When the same assumption is used, the enthalpy of this transition is smaller than would be expected (0.4 vs. 1.0 cal g^{-1}), given that the hinge comprises approximately one-third of long S-2. Measurements of optical rotation show a gradual decrease in molar rotation starting at 10–15 °C which, as was noted earlier, likely corresponds to this transition. Although our heat capacity profiles began between 5 and 10 °C, it is difficult to separate the gradual increase in slope due to the onset of a broad transition from the inherently positive slope of the base line. Thus, our estimate of the enthalpy could be too low and correspondingly our estimate of the size of the hinge too small. It is possible that the enthalpy of the hinge is inherently low due to a poorly formed coiled-coil structure. We cannot decide between these two possibilities.

This minor transition is absent in short S-2 while the major transition appears with no perturbation of the T_m, which is in agreement with the optical measurements of Sutoh et al. (1978). Since the primary difference between long and short S-2 is the absence of the hinge region, it is reasonable to assign the endotherm at 41 °C to this structural domain and the major transition to the remainder of coiled-coil structure.

Earlier studies have estimated the size of the cooperative unit giving rise to the major transition to be ~80 residues per chain by combining the van't Hoff (35 000 cal mol^{-1}) and calorimetric enthalpies (2 cal g^{-1}; C. A. Swenson, unpublished results) (Harrington, 1979a,b). In the present studies, the enthalpy of the major transition of long S-2 ranged from 2.2 cal g^{-1} at pH 7.4 to 3.5 cal g^{-1} at pH 6.6 in 0.2 M KCl. At pH values less than 6, the apparent enthalpy decreased. This likely is related to aggregation which occurs as the isoelectric point is approached. Determination of the van't Hoff enthalpy from the progress curve derived from the calorimetric trace for the major transition of long S-2 at pH 7.4 yields a value of 90 000 cal mol^{-1}. This is significantly larger than the 35 000 cal mol^{-1} obtained by spectroscopic methods. This discrepancy is likely due to the contribution of the small transition to the transition width in the spectroscopic analysis. Combination of the calorimetric ΔH and ΔH_{vh} as obtained from the calorimetric progress curve suggests a cooperative unit for the major transition of 36 000 g mol^{-1}, which is twice as large as was previously obtained. Since the transition width decreases and the area of the endotherm increases with increases in T_m, ΔH_{vh} and ΔH_{cal} increase simultaneously, suggesting that the size of the cooperative unit is constant. A similar analysis for the transition of short S-2 yields ΔH_{vh} and ΔH_{cal} values which agree within experimental error. This indicates that in short S-2 unfolding is approximated by a two-state transition.

In spite of convincing correlations between relaxation rates of mechanical transients observed in muscle fibers and rates of the helix–coil transition for the major endotherm in S-2, it is unclear as to how to associate the conformational transitions with the generation of tension. The conformational transition observed in these studies and assigned to the hinge region of S-2 is in many ways more attractive as the transducing element in the Harrington model than the major conformational transition studied earlier. Locating the transducing element in the hinge leaves the remaining coiled-coil structure intact to provide sites for interaction with the thick filament. The T_m of the transition in the hinge region of isolated S-2 is in the physiological range, and it is likely that it would be only slightly more stable in vivo. In the context of the Harrington helix–coil model, the hinge would be stabilized in the coiled-coil form by interactions with the thick filament near the S-2–S-1 junction which, if sensitive to the binding of S-1 to actin, could provide coupling of hydrolysis to the conformational transition.

Acknowledgments

We thank Thong Nguyen for technical assistance with these studies.

References

Balint, M., Sreter, F. A., & Gergely, J. (1975) *Arch. Biochem. Biophys. 168*, 557–566.

Burke, M., Himmelfarb, S., & Harrington, W. F. (1973) *Biochemistry 12*, 701–710.

Godfrey, J. E., & Harrington, W. F. (1970) *Biochemistry 9*, 886–893.

Goodno, C. C., & Swenson, C. A. (1975a) *Biochemistry 14*, 867–872.

Goodno, C. C., & Swenson, C. A. (1975b) *Biochemistry 14*, 873–877.

Goodno, C. C., Harris, T. A., & Swenson, C. A. (1976) *Biochemistry 15*, 5157–5160.

Harrington, W. F. (1971) *Proc. Natl. Acad. Sci. U.S.A. 68*, 685–689.

Harrington, W. F. (1979a) *Proteins 4*, 245–409.

Harrington, W. F. (1979b) *Proc. Natl. Acad. Sci. U.S.A. 76*, 5066–5070.

Harvey, S. C., & Cheung, H. C. (1977) *Biochemistry 16*, 5181–5187.

Highsmith, S., Kretzchmar, K. M., O'Konski, C. T., & Morales, M. F. (1977) *Proc. Natl. Acad. Sci. U.S.A. 74*, 4986–4990.

Huxley, A. F., & Simmons, R. M. (1971), *Nature (London) 233*, 533–538.

Huxley, H. E. (1969) *Science (Washington, D.C.) 164*, 1356–1366.

Huxley, H. E., & Hanson, J. (1954) *Nature (London) 173*, 973–976.

Jackson, W. M., & Brandts, J. F. (1970) *Biochemistry 9*, 2294–2301.

Jacobson, A. L., & Henderson, J. (1973) *Can. J. Biochem. 51*, 71–79.

Kielley, W. W., & Bradley, L. B. (1956) *J. Biol. Chem. 218*, 653–659.

Kielley, W. W., Kalckar, H. M., & Bradley, L. B. (1956) *J. Biol. Chem. 219*, 95–101.

Kirschner, K., & Bisswanger, H. (1976) *Annu. Rev. Biochem. 45*, 143–166.

Lowey, S., Slayter, H. S., Weeds, A. G., & Baker, H. (1969) *J. Mol. Biol. 42*, 1–29.

McLachlan, A. D., & Stewart, M. (1975) *J. Mol. Biol. 98*, 293–304.

Potekhin, S. A., & Privalov, P. L. (1978) *Biofizika 23*, 219–223.

Potekhin, S. A., Trapkov, P. L., & Privalov, P. L. (1979) *Biofizika 24*, 46–50.

Privalov, P. L., & Khechinashvili, N. N. (1974) *J. Mol. Biol. 86*, 665–684.

Sutoh, K., Sutoh, K., Karr, T., & Harrington, W. F. (1978) *J. Mol. Biol. 126*, 1–22.

Tsong, Y. T., Karr, T., & Harrington, W. F. (1979) *Proc. Natl. Acad. Sci. U.S.A. 76*, 1190–1113.

Weeds, A. G., & Taylor, R. S. (1975) *Nature (London) 257*, 54–56.

Weeds, A. G., & Pope, B. (1977) *J. Mol. Biol. 111*, 129–157.

Young, D. M., Himmelfarb, S., & Harrington, W. F. (1965) *J. Biol. Chem. 240*, 2428–2436.